Penetration and Breakup of Liquids in Subsonic Airstreams

Joseph A. Schetz* and Atul Padhye†
Virginia Polytechnic Institute and State University, Blacksburg, Va.

An experimental study of the penetration and breakup of liquid jets injected normal to high subsonic speed ($M=0.45$ and 0.75) airstreams through injection ports of various geometries and sizes is reported. The measurement techniques were primarily optical, employing 2.5×10^{-3}-sec photos to produce "streak" pictures for penetration measurements and 10^{-6} and 10^{-8}-sec spark photos to show the details of the breakup process and some droplet size measurements. The penetration data were successfully correlated using groupings of the variables and parameters suggested by a simple analysis.

Nomenclature

A_j	= injector area
b	= dimension of parallel-sided portion of injector
C, C_1, C_2, etc.	= constants
C_d	= discharge coefficient
C_D	= drag coefficient
d	= injector diameter
d_0	= droplet diameter
d_{eq}	= equivalent injector diameter
d_f	= frontal injector dimension
d_s	= sidewise injector dimension
h	= penetration distance
H	= streamwise component of drag
k, k_1, etc.	= constants
M_∞	= freestream Mach number
$\dot{m}$	= mass flow rates
P	= pressure
$\bar{q}$	$=\rho_j V_j^2/\rho_\infty V_\infty^2$ = momentum flux ratio
V	= velocity
ρ	= density
γ	= ratio of specific heats

Introduction

THE problem of predicting the behavior of liquid jets injected into a high-speed airstream has attracted the attention of many researchers due to its wide variety of applications. These include side-force attitude control, thrust-vector control, transpiration cooling of re-entry vehicles in order to provide local cooling in the region of communication antennae to alleviate the "black-out" period, and perhaps most important of all, injection and burning of liquid fuels in ramjet combustors and "dump" combustors. Many of the applications involve devices moving at supersonic speeds; however, the flowfield near the injector may or may not be supersonic. Even though a re-entry vehicle enters the Earth's atmosphere at hypersonic speeds there is a region of subsonic speeds behind the bow shock, and the coolant liquid may be injected in this region. In conventional ramjets, air is captured and decelerated to a subsonic velocity by an inlet diffuser before fuel is added to the airstream. Such applications and others require the study of liquid jets injected across high subsonic speed airstreams.

The oldest work in this field is concerned with low airspeeds in the essentially incompressible regime. The concept of supersonic combustion ramjets triggered the study of the behavior of liquid jets injected into supersonic airstreams, and many data are now available for this case (e.g., Refs. 1-10). There are relatively few data available for transverse liquid jets in high subsonic or transonic speed airstreams. A more extensive discussion of the literature is given in Ref. 11.

The present study was aimed primarily at the ramjet and "dump" combustor applications, however the results should also be useful in other applications. The work was organized to determine the effect of: shape, size, and orientation with respect to the airstream of the injector on the overall penetration; structure of the jet column; droplet size distribution; and possible existence of a liquid surface layer. The main motivation for the work comes from that of Kush and Schetz[9] and Joshi and Schetz,[10] who observed that a liquid jet injected normal to a supersonic airstream through a rectangular slot aligned with the freestream gives significantly higher penetration than through a circular port of the same area.

Although most of the present study involved experimental work, a small theoretical investigation aimed at determining correlation variables was also carried out. In the experimental investigation, gross (macroscopic) properties of the liquid jet (e.g., penetration) were studied through relatively long-exposure wide-view photographs of the jet. The "microscopic" properties such as the structure of the jet and the droplet size distribution were studied using two types of short-exposure photomicrographs. Any theoretical work could also be classified as "macroscopic" and "microscopic." In a "microscopic" analysis, one may take into account details such as the breakup mechanism, whereas, in a "macroscopic" approach, one would consider the entire jet and the liquid particles to be enclosed in a control volume and then apply simple physical laws to obtain an integral picture of jet. This was the viewpoint employed here.

The experimental apparatus, instrumentation and techniques are described first. This is followed by a short presentation of the correlation analysis. The results and conclusions are given as the last sections of the paper.

Experimental Apparatus and Instrumentation

Test Facility

Tests were carried out in the VPI&SU 9-in. × 9-in. supersonic/transonic blowdown wind tunnel. The test section of this basically supersonic tunnel was modified to obtain variable Mach number, subsonic flow. A downstream, adjustable "flapper" valve throat can be adjusted to give any value of Mach number between about 0.2 and 0.i in the constant area test section. Calibration of the test 8 section in the direction transverse to the flow direction showed a uniform velocity distribution over the entire cross section.

Presented as Paper 77-201 at the AIAA 15th Aerospace Sciences Meeting, Los Angeles, Calif., Jan. 24-26, 1977; submitted Jan. 25, 1977; revision received July 5, 1977.

Index categories: Multiphase Flows; Airbreathing Propulsion.

*Professor and Chairman, Aerospace and Ocean Engineering Dept. Associate Fellow AIAA.

†Graduate Assistant. Student Member AIAA.

Freestream Mach numbers of 0.45 and 0.75 were used during this test schedule. The stagnation temperature was at ambient atmospheric value in all of the tests. The stagnation pressure of the freestream was held at 24.4 psia for $M_\infty = 0.75$ and at 30.0 psia for $M_\infty = 0.45$.

Flat-Plate Model

The injection experiments were carried out over a 4-in. × 5-in. flat plate with a rounded, wedge-type leading edge. The plate was mounted on a sting and was located approximately at the center of the test section. The orifice was located 2 in. downstream of the leading edge of the plate. The injectors were in the form of interchangeable brass inserts which fitted through the flat plate forming an orifice flush with the surface. Each injector had a smooth conical entry passage followed by a 1/16-in. straight run. A 1-in.-i.d. plenum chamber was fitted to the plate underneath the injector. This plenum chamber size was large compared to the orifice size, and the pressure in the plenum chamber could be assumed to be equal to the injectant stagnation pressure. Three static pressure taps were located on the plate surface, and two pitot tubes were attached to the side of the model to measure total pressure.

Injectors of two different geometries, circular and slots with circular corners, were used. Rounding of the corners gives more uniform flow of the injectant over the whole area of the slot. Table 1 gives a list of injectors and the test conditions investigated.

Injection System

The injectant was stored in a reservoir which was pressurized by means of compressed air. The injectant, under pressure, would flow through a needle valve, then through a solenoid valve, and, finally, through a Rotameter-type flowmeter before entering the plenum chamber in the model. Since our previous work at supersonic speeds[7] and that of others[8] indicated that fluid properties did not have a significant effect on penetration and breakup, this test program was conducted using water.

Photographic Techniques

Streak Photographs

Streak photographs are relatively long-exposure photographs (2.5 msec) which give time-averaged pictures of the highly unsteady jet. Such pictures were used for the measurements of the penetration. The pictures were taken at a magnification of 3.24:1 provided by an 8-in. focal length, f2 lens. A mercury arc lamp was used as a continuous source of light which was reflected from a parabolic mirror to obtain a parallel beam incident on the jet. The camera was a simple bellow-box arrangement using a Polaroid sheet film holder, (Type 57, 3000 ASA), at the focal plane.

Spark Shadowgraphs

To obtain microscopic details of the jet column and the breakup process, stop-action photographs are required. The exposure time limitation is determined by the type of details desired. In the present investigation, two types of short-exposure photographs were employed.

First, short-exposure photographs with a strobe flash unit giving an exposure time of the order of 0.8 μsec were used. On the other side of the jet, the same camera arrangement as used for obtaining streak photographs was set, but now the shutter was left open. The photographs obtained using this procedure show details of the jet and are useful in studying the wave pattern on the jet surface and the breakup mechanism of the jet.

Second, spark shadowgraphs with an extremely short exposure time (approximately 15 nsec) and magnification of 3.25:1 were obtained with a nanolamp. The optical arrangement for obtaining these is similar to that used for spark shadowgraphs. These photographs show microscopic details of the jet such as droplets and, hence, are used to obtain data about droplet size. Figure 1 shows a typical back-lighted photomicrograph.

Top View Photographs

To search for a liquid layer in the vicinity of the injection port such as was found for supersonic airstreams,[9,10] the flat-plate model was mounted vertically, and front-lighted streak pictures looking down at the jet were taken. An ordinary projector lamp was used as a light source. The camera arrangement was the same as for back-lighted streak photographs.

Analysis for Correlation Parameters

In the present work, a "macroscopic" view of the theoretical analysis was emphasized. Gross aspects of the jet behavior such as penetration are given the main consideration, and the details of the jet structure and unsteadiness are not explicitly considered. The jet and the clumps of the liquid broken from the jet are imagined to be enclosed in a control volume which presents an obstacle to the freestream. This approach neglects the effects of vaporization and hence, may not work well with high-vapor-pressure injectants. This simple analysis is designed to yield the functional dependence of penetration on injectant variables and injector geometry.

Figure 2 shows the control volume used in the analysis of penetration. The face S of the control volume is normal to the freestream direction and sufficiently downstream, so that the liquid particles have attained freestream velocity.

The liquid jet being three dimensional, the drag force N acts perpendicular to the jet trajectory. The component of this force normal to the freestream acts downward and dissipates the normal momentum of the jet.

Table 1 Injectors[a] and test conditions

Test conditions: Crossflow Mach numbers = 0.75 and 0.45; crossflow total temperature = ambient; injectant—water; temperature of injectant—room temperature.

	Rectangular			Circular	
Inj. no.	Width, d	Parallel-sided length, b	Total length, L	L/d	Diam.
1	...	...	...		1/8
2	0.0665	0.133	0.199	3	...
3	0.0506	0.203	0.253	5	...
4	...	...	...	...	3/32
5	0.0498	0.0995	0.149	3	...
6	0.0380	0.152	0.190	5	...
7	...	...	...	...	1/16
8	0.0332	0.0664	0.0996	3	...
9	...	...	...	...	1/32

[a] All dimensions in inches.

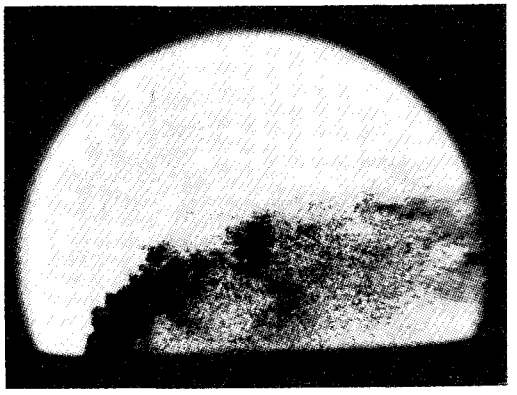

Fig. 1 Representative back-lighted photomicrograph (15 nsec).

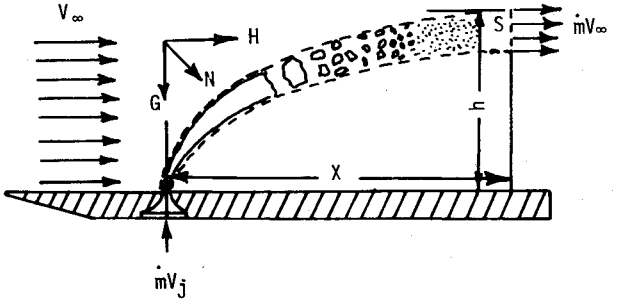

Fig. 2 Control volume for jet penetration.

The rate of change of streamwise momentum of the jet for given freestream conditions is equal to the streamwise component of the drag force N. Thus,

$$H = \tfrac{1}{2}\rho_\infty V_\infty^2 S_f C_D = \dot{m} V_\infty \tag{1}$$

Here C_D is the drag coefficient of the obstacle presented by the control volume which will be called an "equivalent body" hereafter. S_f is the frontal projected area of the jet. Now, let it be assumed that the frontal area S_f is proportional to the product hd_f, where h is the penetration defined as the maximum physical distance the liquid jet penetrates into the freestream and d_f is the frontal linear dimension of the injector. Therefore,

$$S_f = C_1 h d_f \tag{2}$$

Where C_1 is a constant of proportionality and

$$\dot{m} = [(C_1/2)\rho_\infty V_\infty C_D] h d_f \tag{3}$$

C_D is a function of the freestream Mach number and the shape of the equivalent body, which is a function of the injectant properties, injection pressure, freestream conditions, and the injector geometry. Hence, for given injectant and freestream conditions, the equivalent body shape and its size will be functions of only injector geometry and injection pressure. It is expected that injector geometry will govern the shape of the equivalent body, and the size of the injector and changes in the injection pressure will affect only the size of the equivalent body. By definition, C_D depends on the equivalent body shape and not on the size. Altogether, this implies that for a given Mach number of the freestream, C_D is the same for all injectors of the same shape and orientation with respect to the freestream. This shows that for given freestream conditions and for a given shape of the injector,

$$(C_1/2)\rho_\infty V_\infty C_D = C_2 \tag{4}$$

Hence, Eq. (3) becomes

$$C_2 h d_f = \dot{m} \tag{5}$$

i.e.,

$$h d_f \propto \dot{m} \tag{5a}$$

This result is intuitively obvious, since for a given injector and orientation with respect to the freestream, higher $\dot{m}$ means higher normal momentum of the jet as it comes out of the injector and, hence, larger penetration. Later, the experiments will verify the validity of Eq. (5), thereby tending to justify the underlying assumptions.

Next, the penetration will be related to the customary variable of jet/freestream dynamic pressure ratio $\bar{q}$ and to injector geometry. By definition of $\bar{q}$ and $\dot{m}$ we can write

$$\bar{q} = \frac{\dot{m}^2}{\rho_\infty V_\infty^2 \rho_j A_j^2 C_d^2} \tag{6}$$

Substituting for $\dot{m}$ from Eq. (5)

$$\frac{h}{d_f} = \text{const}\left(\frac{\rho_j}{\rho_\infty}\right)(\bar{q})^{1/2}\left(\frac{C_d}{C_D}\right)\left(\frac{d_{eq}}{d_f}\right)^2 \tag{7}$$

Since C_D is unknown, it can be combined with other known quantities to form an undetermined constant C for a given (ρ_j/ρ_∞) such that

$$\frac{h}{d_f} = C(\bar{q})^{1/2} C_d \left(\frac{d_{eq}}{d_f}\right)^2 \tag{8}$$

Since C includes C_D, note that it is a function of injector shape.

Starting again with the definition of $\bar{q}$ and using measurable quantities

$$\bar{q} = \frac{2}{\gamma M_\infty^2}\left(\frac{P_{oj}}{P_\infty} - \frac{P_l}{P_\infty}\right) \tag{9}$$

where P_l is the static pressure at the base of the jet. At the base, the jet itself is approximately normal to the freestream, and hence, P_l can be said to be approximately equal to the freestream static pressure since the freestream is subsonic. Combining Eqs. (8) and (9), we get

$$\frac{hM_\infty}{d_f} = \text{const}\sqrt{\left(\frac{\rho_j}{\rho_\infty}\right)}\left(\frac{P_{oj}}{P_\infty} - \frac{P_l}{P_\infty}\right)^{1/2}\left(\frac{C_d}{C_D}\right)\left(\frac{d_{eq}}{d_f}\right)^2 \tag{10}$$

where "const" has absorbed the effect of γ.

The following observations can be made from this result:

1) For given freestream conditions and injector geometry, C_D can be assumed to be constant and:

a) penetration is proportional to the square root of the injection pressure (note that $P_{oj}/P_\infty \gg P_l/P_\infty$).

b) penetration is proportional to the square root of the injectant density when injectant pressure is constant.

2) For a given injector geometry and injection pressure, the effect of the freestream condition is:

a) penetration decreases with an increase in the freestream Mach number. (Although C_D is roughly constant over a wide range of subsonic Mach numbers, it increases sharply as transonic Mach numbers are reached. This further decreases the penetration.)

b) penetration decreases with an increase in the freestream static pressure and the freestream density when the freestream stagnation pressure is held constant. Alternately, if freestream stagnation pressure is held constant and the stagnation temperature is increased, the penetration will also increase.

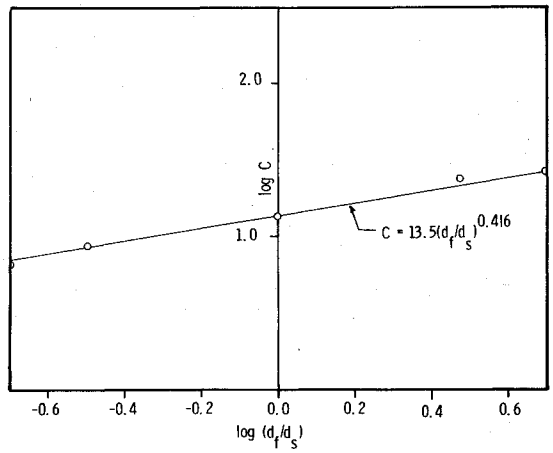

Fig. 3 Log C vs log (d_f/d_s).

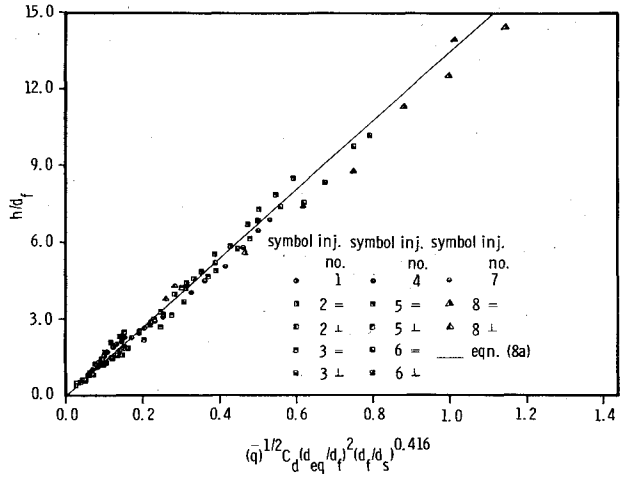

Fig. 4 Penetration correlation for all injectors tested.

Results

Jet Penetration

As mentioned before, the longer-exposure, streak photographs were used for measuring penetration. Penetration is a function of x downstream of the injector and assumes an asymptotic value as the jet loses its normal momentum. In the present work, all of the measurements were taken at $x/d=6.25$ downstream of the center of the injector. This distance was sufficient for the jet to attain essentially its asymptotic value of penetration.

Measured penetration was first plotted against measured mass flow rate of injectant for different values of d_f/d_s. Next, plots were made of nondimensional penetration h/d_f vs nondimensional injectant flow, $\bar{q}^{1/2} C_d (d_{eq}/d_f)^2$. These give a family of curves with parameters, d_f/d_s.

As developed in the foregoing, the equation of nondimensional penetration for given injectant and freestream conditions is Eq. (8). If the injector shapes are characterized by d_f/d_s, then $C=f(d_f/d_s)$. According to Eq. (8), C is the slope of the curve h/d_f vs $(\bar{q})^{1/2} C_d (d_{eq}/d_f)^2$ so that C can be found out from the plots. It was assumed that

$$C=c_3 (d_f/d_s)^{c_4} \tag{11}$$

where c_3 and c_4 are constants. The data fit this assumption yielding

$$C=13.5 (d_f/d_s)^{0.416} \tag{12}$$

The adequacy of this curve fit can be seen in Fig. 3 for a few typical cases. When this form of C is substituted in Eq. (8), we get

$$\frac{h}{d_f}=13.5(\bar{q})^{1/2} C_d \left(\frac{d_{eq}}{d_f}\right)^2 \left(\frac{d_f}{d_s}\right)^{0.416} \tag{8a}$$

The penetration data for all the injectors and all test conditions cluster around a single straight line defined by Eq. (8a) as seen in Fig. 4.

Effect of Injector Shape

In combustion applications, a definite amount of fuel is added to the airstream to achieve the desired fuel/air ratio. The main concern is to achieve proper mixing of the fuel and air, and this is determined by penetration and droplet size. For a given mass flow rate, the penetration is governed by injector shape. To display this, substitute for $\bar{q}$ in Eq. (8a) to get

$$h=k \frac{\dot{m}}{\rho_\infty^{1/2} \rho_j^{1/2} V_\infty} (d_f/d_s)^{0.416} \frac{1}{d_f} \tag{8b}$$

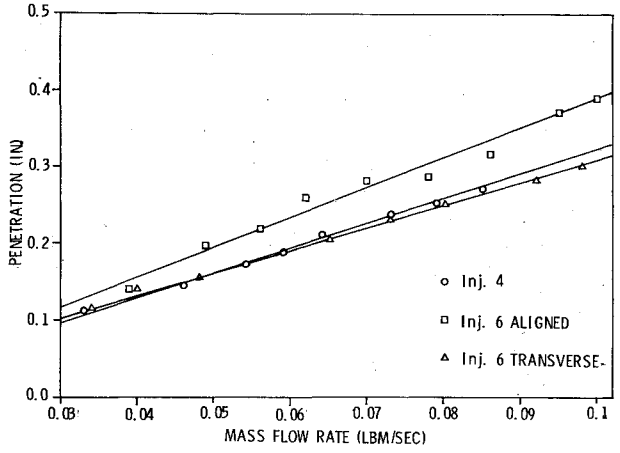

Fig. 5 Comparison of circular and rectangular injectors having same area.

If a circular injector is considered,

$$d_f=d_s=d_{eq} \text{ and } h_{circ}=\frac{k_1}{d_{eq}}$$

Next, consider an injector of rectangular geometry with $d_f/d_s=1/5$, the same area as the foregoing circular injector and aligned with the freestream, then

$$h_{align}=1.26k_1/d_{eq}$$

If the same rectangular injector is placed in a transverse orientation, then $d_f/d_s=5$, and

$$h_{trans}=0.96\, k_1/d_{eq}$$

This shows that for these conditions; $h_{aligned} > h_{circ} \geq h_{transverse}$. It should be noted that the difference between h_{circ} and $h_{transverse}$ is not large for this case. These results can be clearly seen for the case plotted on Fig. 5. Taken with the other cases studied, we can conclude that, in general, $h_{aligned} > h_{circ} \geq h_{transverse}$.

Effect of Injector Size of Given Shape

For a given injector shape, d_f/d_s, C_D can be assumed to be constant when M_∞ is constant. For these conditions, Eq. (8) becomes

$$h=\text{const}\ (\dot{m}/d_f)$$

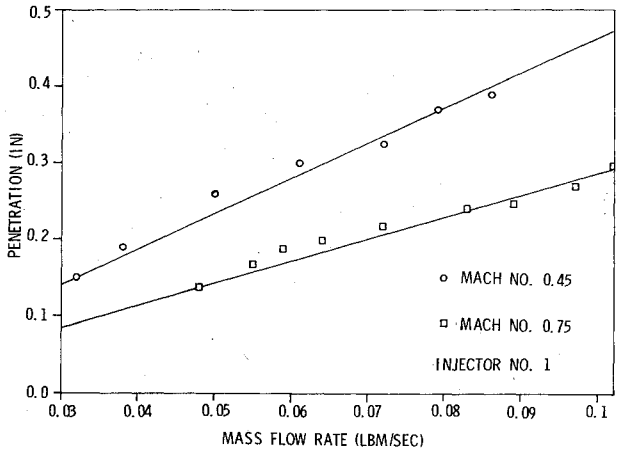

Fig. 6 Effect of freestream Mach number on penetration.

i.e., for a given mass flow rate, penetration is inversely proportional to the frontal dimension.

Effect of Freestream Mach Number

As mentioned before, penetration decreases with an increase in the freestream Mach number. This can be seen from Fig. 6, which shows penetration vs mass flow rate for a given injector for two different subsonic Mach numbers.

The correlation equation developed for supersonic airstreams in Ref. 10 that corresponds to Eq. (8a) had a lower proportionality constant (5.75 as opposed to 13.5 here) and a slightly different exponent on the parameter, d_f/d_s (0.46 as opposed to 0.42 here). The largest effect of a supersonic airstream on penetration is clearly due to the substantially decreased value of the proportionality constant. This can be attributed to the generally higher drag coefficient to be expected for flows over bluff bodies at supersonic speeds.

Jet Breakup

A qualitative study of the effect of injector geometry on jet breakup and instantaneous structure was carried out. In the present investigation, back-lighted photomicrographs with two different exposure times were used to obtain this information. The spark photographs (0.8 μsec) were the primary data used to show wave structure and breakup. Figures 7a-c show typical examples.

The following observations were made from the spark shadowgraphs: 1) the axial distance to the gross fracture increases with increases in $\bar{q}$; 2) with an increase in $\bar{q}$, the amplitude and the wavelength of surface waves reduces; 3) the effects of injector geometry for given $\bar{q}$ were that the axial distance to the fracture is largest for an aligned rectangular slot and least for the transverse slot, and clump size is largest for the rectangular slot in the aligned orientation and smallest for the transverse orientation.

Droplet Size Measurements

The measurements of droplet size were made using a microscope with magnification of 62.5 with the 15-nsec photographs. All of the measurements were made at a plane normal to the freestream at a downstream distance of $x/d_{eq} = 6.25$. The sample back-lighted photomicrograph in Fig. 1 shows a darker core along the center line of the jet. This is due to the presence of either liquid clumps or masses of liquid droplets indistinguishable from one another. Because of this, droplet size measurements were impossible to make in this region of the jet. Hence, measurements were made only in the region where individual droplets were clearly visible, i.e., at the edge of the core and away from the darker portion. Droplets were not very clear in this region for the lower mass flow rates of the injectant and larger equivalent diameters. Figures 8a and 8b show representative histograms for droplet size.

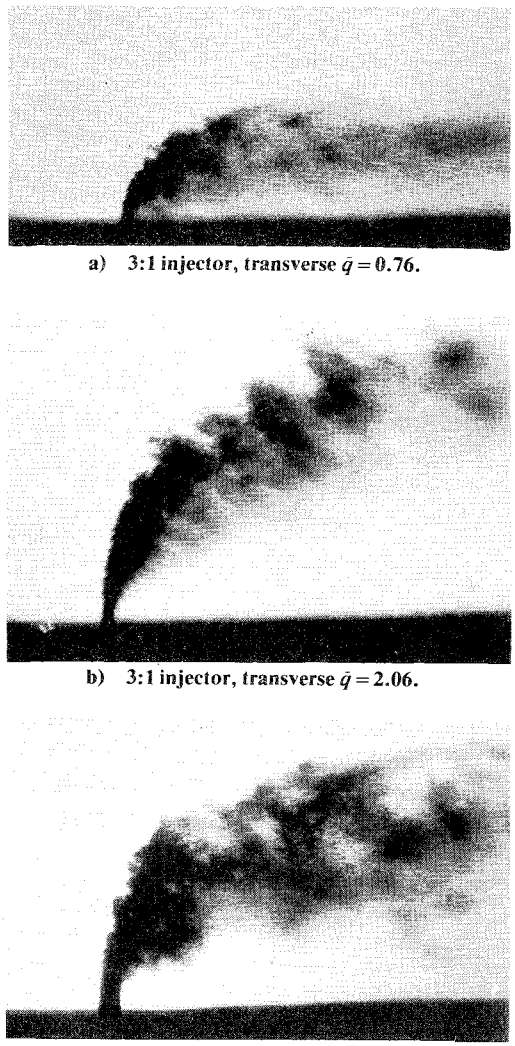

a) 3:1 injector, transverse $\bar{q} = 0.76$.

b) 3:1 injector, transverse $\bar{q} = 2.06$.

c) 3:1 injector, aligned, $\bar{q} = 2.05$.

Fig. 7 Typical back-lighted, spark (0.8 μsec) photographs.

The following observations can be made about the mean drop sizes: 1) the average droplet size was of the order of 10^{-2} in.; 2) for a given injector and freestream conditions, mass flow rate did not affect droplet size greatly; 3) decreasing d_{eq} increased mean droplet size; 4) increasing M_∞ decreased mean droplet size; 5) injector geometry had a major effect on average droplet size. The rectangular injector oriented aligned with the freestream decreased average droplet size whereas, when it was oriented transverse, the average droplet size increased.

Two observations can be made when these results are compared with those of Weiss and Worsham.[12] First, the droplet size as determined in the present investigation is of the order of 10^{-2} in., much larger compared to that measured by Weiss and Worsham which was of the order of microns. This difference in the measured diameters can be explained in the following manner. Here, the sampling plane was at $x/d_{eq} = 6.25$ whereas it was at $x/d_{eq} = 123$ to 218 in the experiments of Weiss and Worsham. It can be argued that the droplets were not fully developed at the time of measurements in the present investigation, and the results might well have been comparable if higher values of x/d_{eq} had been used. Second, the number of droplets investigated in the present study is small compared to that studied by Weiss and Worsham. This is due to a basic weakness of the measuring technique used. In the photographic measuring technique, measurements are made only for a very short duration of time and at a single plane. This gives information about only a few droplets. In

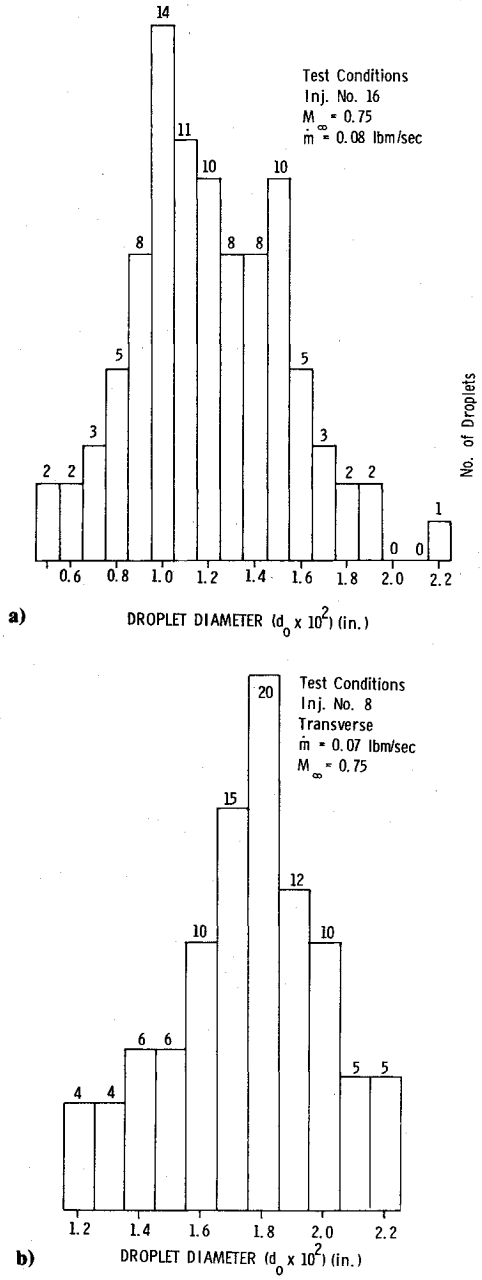

Fig. 8 Droplet size distribution—histogram.

the "hot-wax" method used by Weiss and Worsham, sampling time is large, and a larger number of sample droplets can be obtained. Of course, the "hot-wax" technique has obvious limitations and cannot be generally employed.

Liquid Surface Layer

The top view photographs and visual observations showed that there was no liquid surface layer present near the injection port. The liquid surface layer has been supposed to be a product of shock boundary-layer interaction.[9,10] Since in the subsonic flow there is no shock, no interaction exists, the absence of a liquid surface layer is consistent with this reasoning.

Conclusions

The results of the simple correlation parameter analysis and the experiments yield the following relation for cross-stream penetration:

$$\frac{h}{d_f} = 13.5(\bar{q})^{1/2} C_d \left(\frac{d_{eq}}{d_f}\right)^2 \left(\frac{d_f}{d_s}\right)^{0.416}$$

Specific conclusions as to the effects of freestream Mach number, flow rate, injector size and shape, etc. can be easily determined from this expression. This has been carried out in the main text. One major result was that $h_{align} > h_{circ} \geq h_{trans}$. Our previous work with a supersonic freestream[10] had the last two items reversed and a somewhat more significant difference between them.

Studies of the jet structure and breakup indicated that an increase in $\bar{q}$ increases the axial distance to the gross fracture of the jet and decreases the amplitude and wavelength of the surface waves. The axial distance to the gross fracture is the largest for the aligned rectangular slot and the least for transverse rectangular slot.

On the basis of the limited measurements made at a single station close to the injection port: the mean droplet size was of the order of 10^{-2} in., decreasing d_{eq} increased mean droplet sizes and increasing freestream Mach number decreased mean droplet size. Further work on droplet sizes should probably be based upon some light-scattering or absorption technique to produce a larger body of data. There was no trace of a liquid surface layer near the injection port under any condition tested, and it was concluded that a liquid surface layer does not exist for liquid injection into subsonic flow.

Acknowledgment

This work was supported by the Air Force Office of Scientific Research under AFOSR-74-2584 with B. T. Wolfson as the Project Monitor.

References

[1] Dowdy, M. and Newton, J., "Investigation of Liquid and Gaseous Secondary Injection Phenomena on a Flat Plate with $M=2.01$ to $M=4.54$," Jet Propulsion Lab., TR 32-542, Dec. 1963.

[2] Forde, J., Molder, S., and Szpiro, E., "Secondary Liquid Injection into a Supersonic Airstream," *Journal of Spacecraft and Rockets*, Vol. 3, Aug. 1966, pp. 1173-1176.

[3] Kolpin, M., Horn, K., and Reichenbach, R., "Study of Penetration of a Liquid Injectant into a Supersonic Flow," *AIAA Journal*, Vol. 6, May 1968, pp. 853-858.

[4] Catton, I., Hill, D. E., and McRae, R. P., "Study of Liquid Jet Penetration in a Hypersonic Stream," *AIAA Journal*, Vol. 6, Nov. 1968, pp. 2084-2089.

[5] Horn, K. and Reichenbach, R., "Further Experiments on Spreading of Liquids Injected into a Supersonic Flow," *AIAA Journal*, Vol. 7, Feb. 1969, pp. 358-359.

[6] George, D. J. and Spaid, F. W., "Holography as Applied to Jet Breakup and an Analytical Method for Reducing Holographic Droplet Data," Air Force Rocket Propulsion Lab. TR-72-72, Sept. 1972.

[7] Sherman, A. and Schetz, J., "Breakup of Liquid Sheets and Jets in a Supersonic Gas Stream," *AIAA Journal*, Vol. 9, April 1971, pp. 666-673.

[8] Reichenbach, R. and Horn, K., "Investigation of Injectant Properties on Jet Penetration in a Supersonic Stream," *AIAA Journal*, Vol. 9, March 1971, pp. 469-472.

[9] Kush, E. and Schetz, J., "Liquid Jet Injectant into a Supersonic Flow," AIAA Paper 72-1180, New Orleans, La., Nov.-Dec. 1972.

[10] Joshi, P. and Schetz, J., "Effect of Injector Shape on Penetration and Spread of Liquid Jets," *AIAA Journal*, Vol. 13, Sept. 1975, pp. 1137-1138.

[11] Schetz, J. A., McVey, W., Padhye, A., and Munteanu, F., "Studies of Transverse Liquid Fuel Jets in High-Speed Air Streams," VPI-Aero-049, Virginia Polytechnic Institute and State University, July 1976 (available through DDC).

[12] Weiss, C. and Worsham, C., "Atomization in High Velocity Air Streams," *ARS Journal*, Vol. 29, April 1959, p. 252.